MULTI-EVAPORATOR CLOSED LOOP THERMOSYPHON

M. Mameli[a]* (mauro.mameli@unibg.it), D. Mangini[a](daniele.mangini@unibg.it), G.F. Vanoli[b] (giulio.vanoli@mail.polimi.it), L. Araneo[b] (lucio.araneo@polimi.it), S. Filippeschi[c] (sauro.filippeschi@den.unipi.it), M. Marengo[a,d] (M.Marengo@brighton.ac.uk)
**** corresponding author***
[a] *Università di Bergamo, Viale Marconi 5, 24044 Dalmine (BG), Italy*
[b] *Politecnico di Milano, Dipartimento di Energia, Via Lambruschini 4A, 20158 Milano, Italy*
[c] *Università di Pisa, DESTEC, Largo Lazzarino 2, 56122 Pisa, Italy*
[d] *University of Brighton, School of Computing, Engineering and Mathematics, Brighton BN2 4GJ, UK.*

ABSTRACT
A novel type of multi-evaporator Closed-Loop Two-Phase Thermosyphon has been designed and tested at different inclinations and heat input levels. The device consists in an aluminum tube (I.D./O.D. 3/5 mm), bended into a planar serpentine with five U-turns in the heated zone, with a 50 mm transparent section for the purpose of visualization. The tube is closed in a loop, evacuated and partially filled with FC-72, 50% vol. Each turn is equipped with an electric wiring heater and the peculiar location of the heating sections causes the fluid to circulate regularly in a preferential direction. The condenser zone is embedded into a heat-sink and cooled by fans blowing air at 20 °C. Sixteen T-type thermocouples are located on the external tube wall in the evaporator and condenser zones, while the fluid pressure is measured in the condenser zone adjacent to the transparent tube. The flow pattern is recorded by means of a high-speed camera, the device operational limits (start-up and dry-out heating levels at the different inclinations) are detected and the overall thermal performance is calculated for different inclination angles and heat power inputs. Thanks to the fluid flow motion stabilization in a preferential direction due to the peculiar position of the heating elements, in vertical position the device is able to dissipate heat fluxes higher than 57% with respect to the CHF limit for FC-72, keeping also the temperatures at the evaporator zone lower than 80 °C.

INTRODUCTION
Two phase heat transfer devices have always been attractive for their compactness, high performance and, above all, the possibility of being completely thermally driven (passive). The increasing need of managing high heat fluxes, either to be dissipated (electronics cooling) or to be recovered (solar concentrators), drives toward the design of more efficient and reliable devices. Despite the last decades witnessing the overwhelming spread of the heat pipe technology under various forms such as grooved and sintered heat pipes, loop heat pipes and capillary pumped loops, the interest in wickless, gravity driven technologies, namely the Two Phase Thermo-Syphons (TPTS), never damped out. The capability to transport heat at high rates over appreciable distances, without any requirement for external pumping devices, the low cost, durability and relatively simpler modeling/design process make this technology very attractive for many thermal management applications. Indeed, TPTS have been investigated in plenty of fields such as: nuclear plants *(Lahey and Moody 1993)*, energy systems *(Franco and Filippeschi 2013)*, solar heat recovery *(Esen and Esen, 2005)*, *(Li et al. 2014)*, *(Moradgholi et al. 2014)*, air conditioning *(Han et al. 2013)*, electronic cooling in avionics *(Sarno et al. 2013)* and in railway traction *(Perpinà et al. 2007)*. The typical TPTS *(Reay and Kew 2006)* consists of a single envelope where the heat-receiving (evaporator) zone is usually filled with the liquid phase and it is located below the heat rejecting (condenser) zone. As the evaporator zone is heated up, the liquid starts boiling and vapor rises and condenses on the walls in the heat-rejecting zone. The liquid film flows down by gravity the walls to the evaporator zone counter-current the vapor. At high heating power input, because of the correspondingly large mass flow rate of the vapor, the liquid-vapor interfacial shear stress becomes increasingly relevant. Once the interfacial shear force overcomes the gravitational force on the liquid film, the liquid flow may be reversed and the flooding limit is reached. Many novel designs have been proposed to overcome the flooding limit, which include an internal physical barrier along the adiabatic section by-pass line for liquid return, a cross-over flow separator. The main advantage of these designs is that the liquid and vapor flows have partially separated passages, which can result in a higher flooding-limited heat transfer capacity. Another way to separate phases and increase the device performance is to create a loop where

the fluid is forced to circulate in a preferential direction by the coupled effect of vapor pressure and gravitational force. The present device consists in a relatively small diameter aluminum tube (3 mm ID, 5 mm OD), however higher than the capillary diameter for the used refrigerant (1.6 mm for FC-72 at 20 °C). Indeed, as thoroughly described by *Franco and Filippeschi (2010, 2012)* thanks to the relatively small cross section with respect to the standard TPTS, the expanding vapor phase is able to push batches of fluid (both liquid and vapor) towards the condenser section. In the cooled zone, vapor condenses and the tube is completely filled by the liquid phase that is driven back to the evaporator by gravity. This particular fluid flow motion is better known as "bubble lift" principle. The looped TPTS based on the "bubble lift" concept, exploits the higher heat transfer performance linked to the convective flow boiling process in order to overcome the limits due to the pool boiling critical heat flux. In the field of electronic cooling, the loop thermosyphons are largely investigated because of their geometrical flexibility in the design of the evaporator and the condenser zones with respect to a single straight channel typical of a normal thermosyphon *(Franco and Filippeschi, 2012)*. Indeed, the aluminum tube is bended in a serpentine manner, allowing the device to meet especially electronic cooling requirements. Furthermore, a strategic asymmetric alternation of multiple heating and cooling zones guarantees the fluid circulation in a preferential direction without losing the constructive simplicity, expanding the above concept into a multi-evaporator two-phase thermosyphon. The asymmetrical positions of the heating elements, permitting fluid circulation in a preferential direction, make this device different from the parallel assessments *(Kim et al. 2005)*, *(Kaminaga et al. 2012)* previously studied. Thanks to the self-sustained fluid circulation, the maximum heat flux abundantly exceeds the standard pool boiling limit allowing the device to maintain high performances at even high heat input levels with respect to standard TPTS operated with fluorinerts *(Jouhara and Robinson 2010)*.

EXPERIMENTAL SETUP

The proposed cooling device is made of an aluminum tube (I.D./O.D. 3.0 mm/5.0 mm respectively) bent into a planar serpentine with ten parallel channels and five turns at the evaporator (all axial curvature radii are 7.5 mm), as shown in Figure 1a. The aluminum tube is filled up with a refrigerant fluid (FC-72), utilizing a Filling Ratio FR=50%, corresponding to a liquid volume of 8.3 ml. The thermosyphon has been tested at different heat loads from 10 W up to 260 W and different inclination angles (vertical, 75°, 60°, 45°, 30°, 15°, 5°, 2°, horizontal). A 50 mm glass tube closes the loop at the top of the condenser zone, allowing the flow pattern visualization. The glass tube is connected to the aluminum serpentine by means of two "T" junctions that derive two ports at each side: one is devoted to the vacuum and filling procedures, while the second one hosts a pressure transducer (Kulite®, XCQ-093, 1.7 bar Absolute).

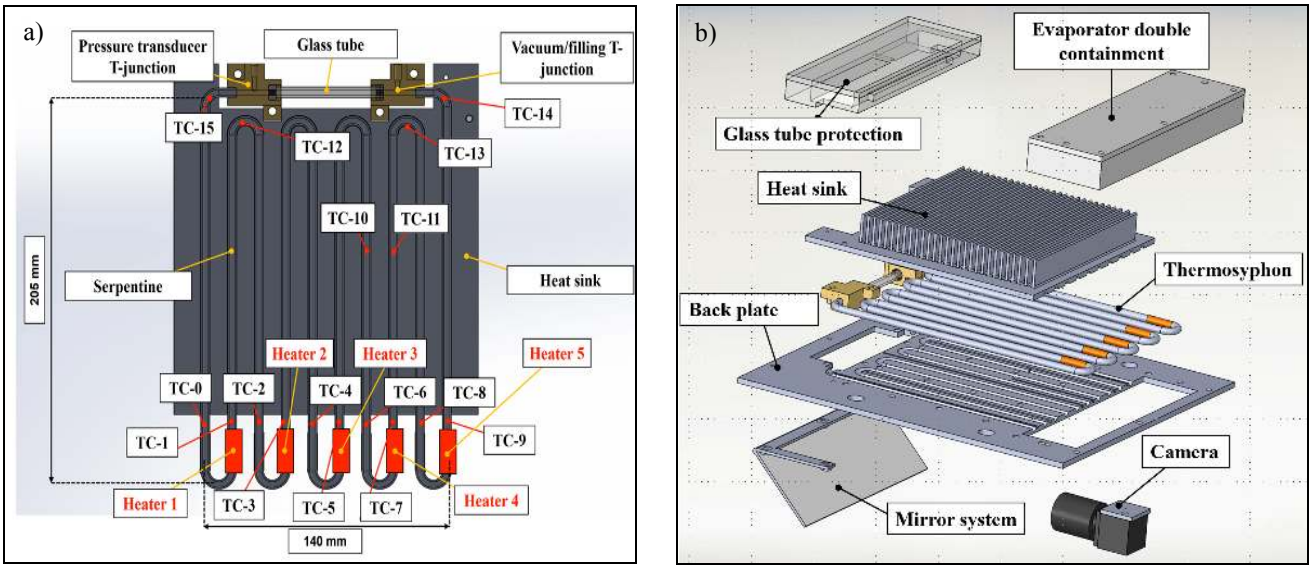

Figure 1. a) Thermocouples and heaters location along the thermosyphon tube; b) Exploded view of the test cell with all its main components.

Sixteen "T" type thermocouples (bead diameter 0.2 mm, ± 0.3 K) are located on the thermosyphon external tube wall: ten in the evaporator zone and six in the condenser zone, while an additional thermocouple is utilized to measure the ambient air temperature as illustrated in Figure 1a. A low vapor-pressure glue (Varian Torr Seal®) seals together the aluminum tube, the "T" junctions and the glass tube.
The exploded view of the test cell, with its main components, is visible in Figure 1b. A compact camera (Ximea®, MQ013MG-ON objective: Cosmicar/Pentax® C2514-M) records the flow patterns within the glass tube. The camera, diminishing the recorded region of interest at the glass tube only, acquires images up to 450 fps with a resolution of 1280x162 pixel (corresponding to a spatial resolution of 25 pixel/mm). The thermosyphon is firstly evacuated by means of a vacuum system Varian® DS42, TV81-T) down to 10^{-6} mbar. Before filling up, the incondensable gases are earlier removed by continuous boiling and vacuum cycles in a secondary tank, as described by Henry et al. [2004]. Finally, the system is filled up with the working fluid (FC-72) utilizing a filling ratio of 0.50 ± 0.03. The difference between the actual fluid pressure inside the tube and its saturation pressure, at the ambient temperature, gives an indication of the incondensable gas content. For the present case this difference is less than the pressure transducer accuracy. Five electrical heaters (Thermocoax® Single core 1Nc Ac, 0.5 mm O.D., 50 Ω/m, each wire is 720 mm long) are wrapped just above the evaporator U-turns (Figure 1a) covering a tube portion of 20 mm and providing an asymmetric heating on the device. A power supply (GWInstek® 6006A) is connected to the heaters, providing an electric power input up to 260 W (corresponding to a wall to fluid radial heat flux of 27 W/cm^2). Steady state conditions can be reached in approximately 3 minutes due to the low thermal inertia of the heating system.

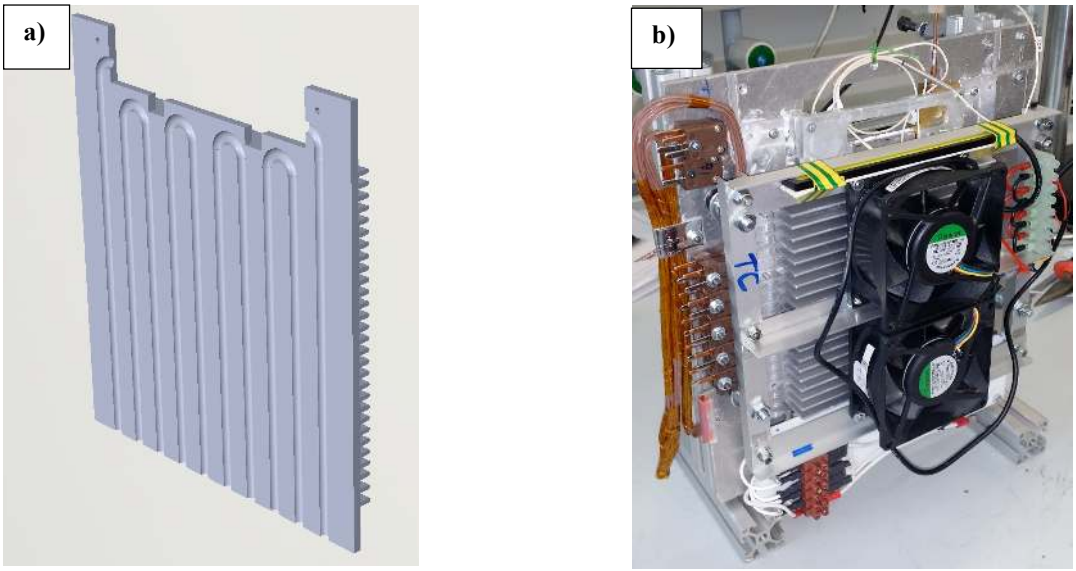

Figure 2. a) CAD view of the milled heat sink; b) The two fans mounted above the heat sink.

In order to increase the condenser surface, the device is embedded between a heat sink and a back plate (Figure 2a) where circular cross section channels are milled. The thermosyphon is cooled down by means of two air fans (Sunon® PMD1208PMB-A), positioned just above the heat sink (165 mm total length), as shown in Figure 2b. The thermal contact between the heat sink, the aluminum back plate and the enclosed thermosyphon is enhanced by the use of thermal conductive paste (RS® Heat Sink Compound). All the tests are performed at controlled ambient temperature (20 °C ± 1 °C). The cooling device, the thermocouples, the pressure transducer, the heating and cooling system as well as the visualization system are installed on a structure that can be easily tilted from the vertical position (bottom heat mode) to the horizontal. The thermocouples and the pressure transducer outputs are recorded by a data acquisition system (NI-cRIO-9073®, NI-9214®, NI-9215®) at 16 Hz. A video sequence (10 seconds at 450 fps) is recorded during each tested combination of heat input power and inclination angle. The video acquisition starts 13 minutes after each heat input power variation in order to reach pseudo-steady state conditions.

EXPERIMENTAL RESULTS

The experimental campaign is carried on in order to identify:

- the temporal evolution of the tube temperature in every branch of the evaporator zone and along the condenser zone;
- the operation regimes in terms of fluid motion;
- the operational limits in terms of heat input levels and orientation;
- the device thermal performance at each input level and orientation.

Indeed, for each inclination, the heater input power is increased in multiples of 10 W steps, with finer detail in the lower power region, until a thermal crisis condition (namely the evaporator dry-out condition) is reached. After the sudden increase of the evaporator temperatures due to the dry-out condition, at the following power step the heating power is reduced and the thermal characterization is continued while decreasing the heat input levels. Each power step is maintained for at least 15 up to 16 minutes so that the system can reach a steady state condition and the equivalent thermal resistance can be evaluated as follows:

$$R_{eq} = \Delta\bar{T}_{e-c} / \dot{Q} \tag{1}$$

where $\Delta\bar{T}_{e-c}$ is the difference between the evaporator and the condenser mean temperatures, averaged in time during the last minute of the pseudo-steady state, and $\dot{Q}$ is the effective heat power input provided to the evaporator zone by the five heaters. Care is taken to allow the liquid to reside evenly among the curves by holding the device horizontal before raising it to the desired inclination.

Thermal characterization in vertical position

Figure 3 shows the history of the tube wall temperature in several locations: the red/yellow lines indicate the temporal evolution of the temperatures in the evaporator zone just above the heater (TC1, TC3, TC5, TC7, TC9); the pink colour lines correspond to the temperatures at the evaporator zone far from the heaters (TC0, TC2, TC4, TC6, TC8); the temperatures recorded in the condenser zone are illustrated with blue colour lines (TC10, TC11, TC12, TC13, TC14, TC15); the ambient temperature is shown in green; finally, the fluid pressure is displayed in grey with the scale reported on the secondary y-axis at the right. The sequence of the heat input levels is indicated at the upper side of the chart.

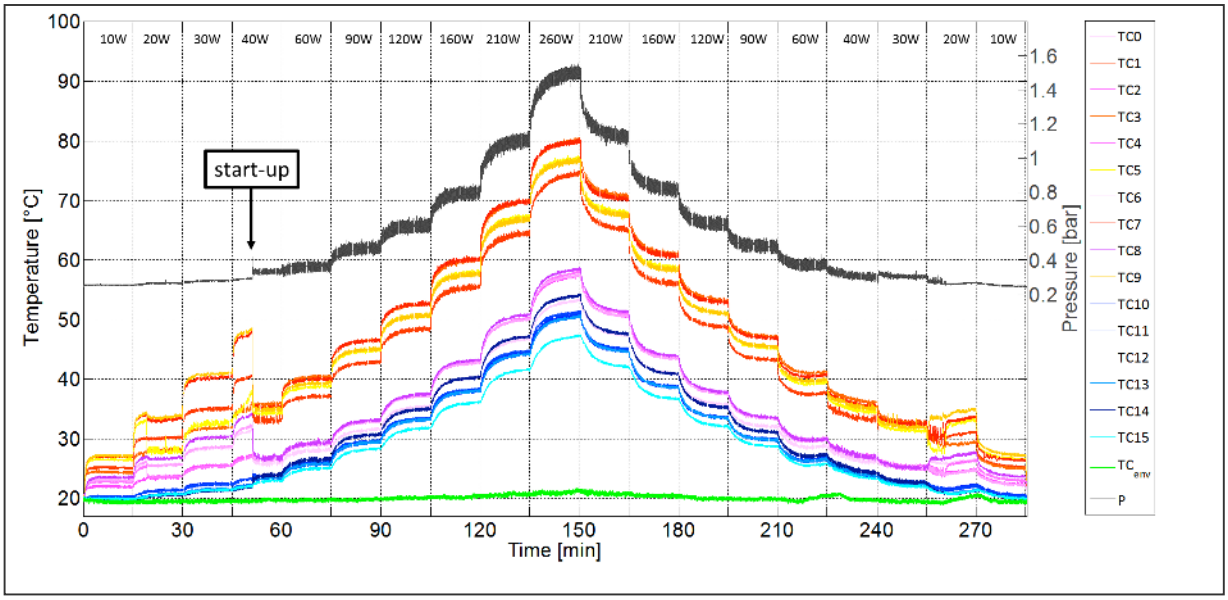

Figure 3. Temperature, pressure and power input diagram in vertical position.

During the first heat input levels (up to 30 W) the fluid is not moving, as evidenced by the smooth pressure signal, and heat is transferred mostly by pure conduction along the tubes. For this reason, even small differences in the thermal contact between the five heating wires and the tube portions can cause a 10 °C temperature spread within the evaporator zone. At 40 W, the device starts up and the regime switches from stationary to circulating almost instantaneously, resulting in a sharp decrease of the temperatures close to the heaters and a noticeable narrowing of the evaporator temperature distribution. In vertical position indeed, thanks to the asymmetrical position of the heaters, the combined effect of vapor bubble-lift and gravity helps the fluid rise up from the heated tubing sections and descend into the cooled sections respectively, as shown in Figure 4.

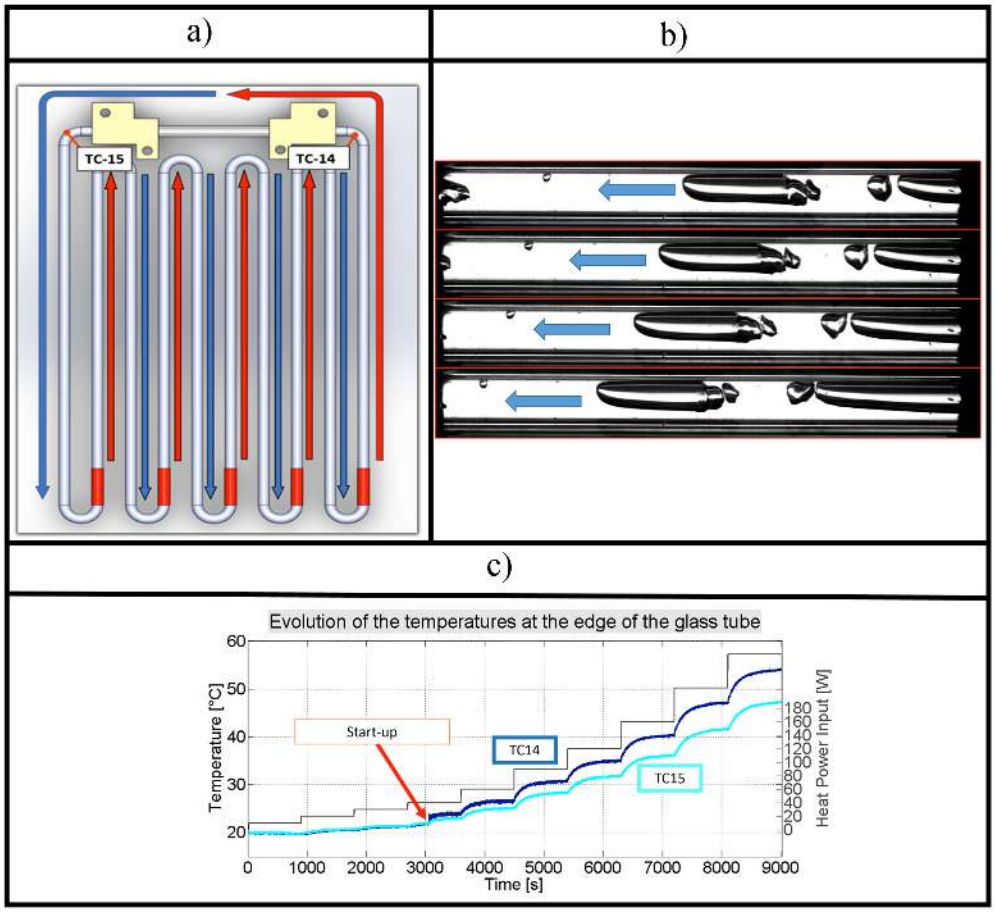

Figure 4. a) Asymmetric heater layout and flow circulation: up-headers highlighted with red arrows; down-comers highlighted with blue arrows; the positions of the TC14 and the TC15 are also indicated; b) Flow circulation at 160 W in vertical orientation; sequence of images at 200 fps; the fluid flow direction is pointed out with blue arrows; c) Evolution of the temperatures at the edges of the glass tube.

In the heated branches (up-headers, highlighted with red arrows in Figure 4a), the fluid batches are lifted up from the evaporator to the condenser in the form of slugs, by means of the expanding vapor bubbles; the gravity head along the adjacent branches (down-comers, highlighted with blue arrows in Figure 4a), assisting the return of the fluid from the condenser down to the evaporator zone, generates a stabilization of the fluid motion in a preferential direction. This can also be observed through the transparent section of the condenser that connects directly the up-header and the down-comer at the right and left sides of the device respectively. During circulation the fluid is always seen going preferentially from left to right of the observation field, as shown in Figure 4b. This net circulation has a direct effect also on the temperatures at the edges of the transparent section in the condenser zone (Figure 4c). During the start-up, the temperatures at the edges of the transparent section are equal, because there is no fluid motion. However, as soon as the fluid starts to reach the condenser zone, TC 14 starts to show values higher than TC 15. This can be explained as follows: the fluid that is pumped from the up-

header reaches the other end with a lower temperature because releases thermal energy during its passage through the T-junctions and the transparent section.
The asymmetrical position of the heaters promotes a stable fluid circulation that allows the device to start up at relatively low power inputs and to dissipate heat fluxes widely beyond the pool boiling Critical Heat Flux (CHF) limits for FC-72 at 80 °C that sets approximately to 17.5 W/cm^2 according to the following correlation *(Katto, 1985)*:

$$Ku = q'' \Big/ \left\{ \Delta h_{lv} \rho_v^{0.5} \left[\sigma g \left(\rho_l - \rho_v \right) \right]^{0.25} \right\} \tag{2}$$

Where Ku is set to 0.14 for the case of pool boiling on an ideally infinite plate. Thusly the device continues to work without reaching any kind of thermal crisis up to the power supply limit of 260 W, corresponding to a tube to fluid radial heat flux of 27 W/cm^2, maintaining the evaporator temperature below 80 °C.
During power-down a flow transition from circulating to oscillating at 30 W is detected, causing the evaporator temperatures to fluctuate. At 20 W, the fluid motion stops altogether, causing the temperature distribution to be again determined by conduction only. The device activation, defined as the onset of continuous fluid motion, occurring at different heat input levels, seems to depend on the heating history (increasing/decreasing heat power levels) thus leading to speculate about the existence of hysteresis in the system: what if the heat input level is again increased? Would the device operation be activated again at 40 W, proving the existence of hysteresis? Or does the flow motion follow the last registered trend, activating at 20 W, testifying only a single start-up phenomenon? In order to answer the previous questions additional tests are performed with three subsequent heating ramps. The device is first heated up through 10 W, 20 W, 30 W, 40 W and 80 W; then it is powered down following the same steps down to 10 W and finally heated up another time up to 80 W. Like the other tests, every power step is held for 15 minutes in order to reach pseudo-steady state conditions and thus have the possibility to calculate the $R_{eq.}$ Figure 5 shows the equivalent thermal resistances in the three different power ramps: the first power-up (Q_{up}), the subsequent power-down with the same power steps (Q_{down}) and finally the second power-up again through the same heating levels (Q_{up2}).

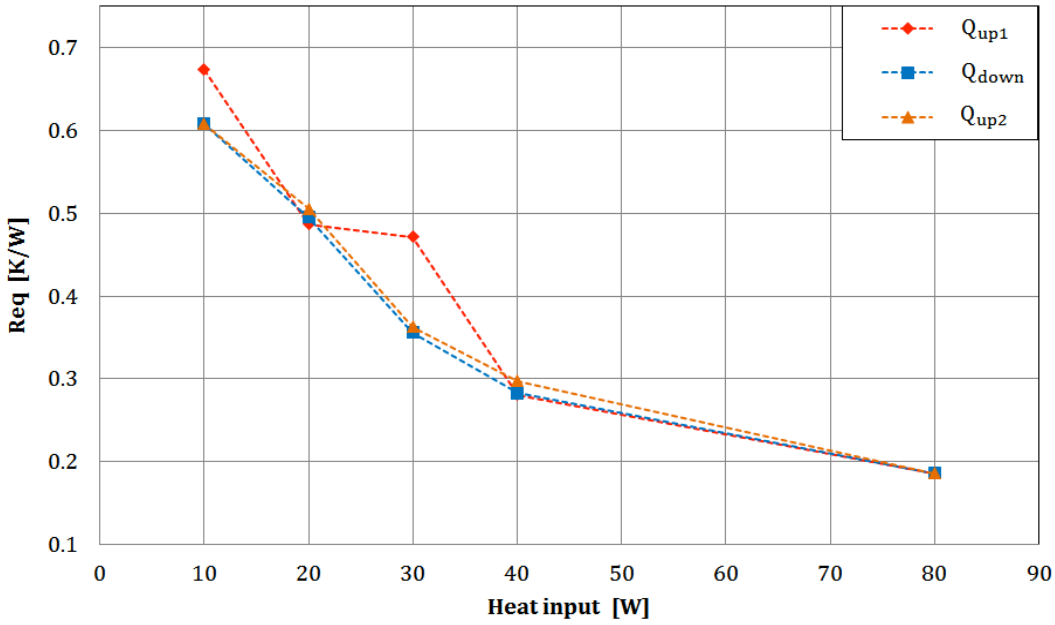

Figure 5. Equivalent thermal resistance during the start-up test.

During the first power-up phase the device start-up is easily recognized in terms of thermal performance by the sudden decrease of the equivalent thermal resistance occurring at 40 W (red line) and confirmed by the absence of visible fluid

motion up to 30 W in the transparent section, while regular motion is detected at 40 W. At 80 W the fluid circulation is fully activated and, during the power-down phase, a residual oscillation is still detected even at 30 W, resulting in a lower thermal resistance with respect to the power-up case. Since the second power-up trend nearly coincides with the power-down, it can therefore be concluded that the difference in performance is not due to hysteresis but just to a single start-up issue. This could be explained as follows: the Q_{up2} part of the test starts from a higher energized condition than the Q_{up}. The nucleation sites, already vigorously activated by the first two ramps (Q_{up} and Q_{down}), are not completely de-activated when the Q_{up2} starts. This situation causes an earlier start-up in the Q_{up2}, allowing the two-phase fluid to move even at 30 W.

Effect of orientation

After the vertical test, other tests at 75°, 60°, 45°, 30°, 15°, 2.5° and another one leaving the device horizontally are performed to evaluate the effect of inclination on the thermal performance of the device. Results are shown in Figure 6a for the power-up case and 6b for the power-down case.

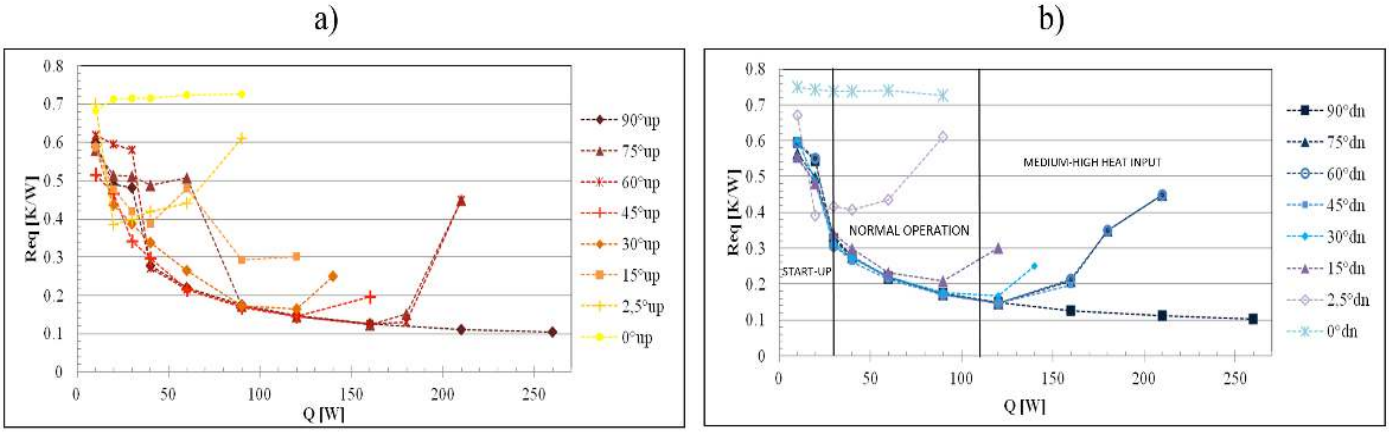

Figure 6. Equivalent thermal resistance at various inclinations. a) The first power-up; b) the subsequent power-down.

Figure 6a shows the power-up phases at every examined inclination, while Figure 6b shows the corresponding power-down phases. In light of the start-up test results, the thermal resistance values registered during the first power-up are only indicative of the device's behavior at start-up. The fact that the liquid phase returns to the condenser more efficiently when the device is fully assisted by gravity (vertical operation) is not valid for the start-up phase, as already shown for other looped two phase passive devices *(Mameli et al. 2013)*. In fact, one could expect that the device start-up may occur at lower heat input levels for lower inclinations but, looking at Figure 6a, it is evident that the start-up heat input ranges from 30 W to 90 W, without a univocal dependence on the tilting angle. On the other hand, in the power down case (Fig. 6b), the fluid motion remains active down to 30 W for all the inclinations, meaning that the liquid phase is pushed back to the condenser more efficiently only when the gravity effect is coupled with fluid inertial effects or, in other words, when the flow motion has already been activated. Therefore, the power-down phase better describes real operative performance and can be further examined to distinguish a power range where the device exhibit a stable operation from one where thermal crisis conditions begin to manifest.

In the horizontal orientation, since the tube diameter is larger than the capillary limit (almost 1.6 mm for FC-72 at 20 °C), the liquid phase always resides in the lower half of the pipe while the vapor phase in the upper one: fluid motion is not assisted by gravity and vapor is never confined between liquid batches. This results in a complete absence of macroscopic fluid motion for all the tested heat input levels, proving that gravitational assistance is required to initiate fluid flow motion and thus to activate the device. Indeed, in horizontal orientation, the heat transfer is mainly due to conduction within the tube wall and the fluid itself and the equivalent thermal resistance keeps constant to the higher value of 0.7/0.8 K/W. This trend is taken as reference point because it basically states that the device is not working at all. A slight inclination with respect to the horizontal position (2.5°) is sufficient to assist the fluid motion and makes the device less sensitive to the above mentioned start-up issues. Indeed both during power-up and power-down the fluid starts oscillating at 20 W: the rising bubbles flatten against the upper side of the tubing and, despite the bubble lift effect being drastically reduced, vapor is able to slide upwards

and contribute to convective cooling. The absence of fluid circulation for all the tested heat inputs results in a higher equivalent thermal resistance with respect to the higher inclinations.
For all the inclinations at the lowest power output setting, 10 W, the system always shows its highest thermal resistance (between 0.5 and 0.7 K/W) because the heating power is never sufficient to activate the fluid motion inside the device and the heat transfer is mainly due to pure conduction.
At medium-low power inputs (the normal operation range in Figure 6b), all experiments show the same performance trend: after the activation, the curves collapse into a narrow band of thermal resistance values and performance can therefore be considered independent of inclination. This indicates that in this range, where fluid circulation is strong, the inertia of the circulating fluid is a much more relevant factor than the effect of inclination. As power is increased, equivalent thermal resistance values continue to gradually decrease until a thermal crisis condition is reached, causing temperatures in the affected sections to rise over 100 °C, noticeably penalizing thermal performance. When the heat flux locally exceeds the CHF, a local dry-out condition occurs meaning that a vapor film that prevents contact between liquid and heated surface. The resulting loss of heat transfer capability causes the local temperature to rise abruptly in at least one channel of the device, significantly increasing the R_{eq}. Since the heating power was especially high when dry-out occurred at 75° and 60°, the last thermal resistance values are only approximations because the power input had to be immediately reduced in order to avoid the risk of burn out of some set-up components. .
On the other hand, inclination clearly dictates the CHF level (medium-high heat input zone in fig. 6b): the 15° configuration is the first one to experience the thermal crisis, at 120 W, then the 30° one at 140 W, 45° at 160 W, 60° and 75° at 210 W, while the vertical setup's limits lie beyond the current equipment limit of 260 W. It is therefore clear that the effect of gravity aids in maintaining fluid motion, especially in the down-comer sections, which bring down the cooled liquid to displace the vapor bubbles being formed in the evaporator: the lower the gravity head, the lower the fluid momentum opposing to the vapor expansion in the down-comer (see Fig. 6a).

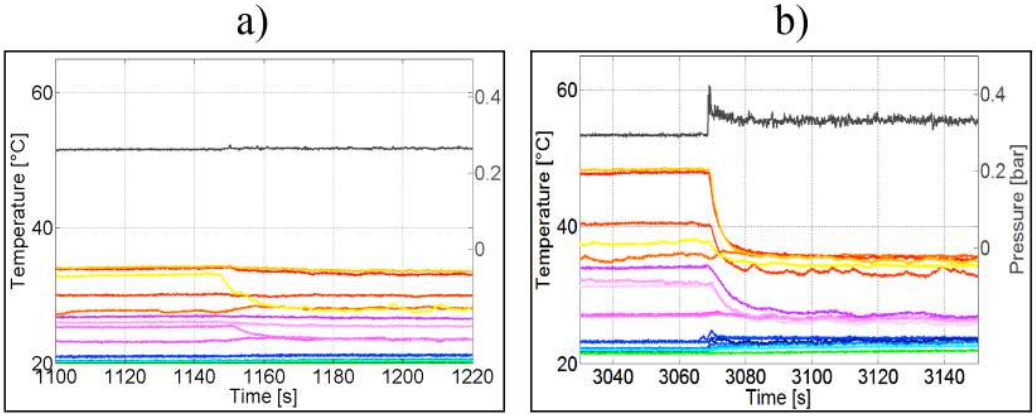

Figure 7. Temperature and pressure during Q_{up} in vertical conditions. a) Partial startup at 30W; b) Complete activation at 40W.

As previously mentioned, the full device operation is reached once stable fluid motion is achieved. This event is always associated with a rapid drop in all evaporator temperatures, an increase in condenser temperatures, a pressure spike followed by sustained pressure oscillation (as seen in Figure 7b). Before that, temperatures may drop in one evaporator curve only (see Figure 7a) without necessarily initiating a visible movement of fluid. This is referred to as a partial start-up or partial activation (indicated as "S" in Table 1 at 90°, 30 W) since the reduction in thermal resistance is relatively small compared to full activation. This operating condition can arise in the low power ranges, both during power-up and power-down; it is however an unstable condition, meaning that even without any change to the power output, the activated sections can also regress back to an inactive condition where local fluid motion stops and temperatures rise back up. During the various stages of operation, several different flow regimes can be observed and distinguished through the transparent tubing section (see Table 1):

- " " no symbol = test not performed;
- "-" = no fluid motion;

- "S" = start-up, shut down (unstable): flow may be stratified or weakly oscillating, with partial activation or deactivation of at least one heated section visible from the temperature readings;
- "O" = oscillating (stable): a strong movement of fluid oscillating back and forth;
- "C" = circulating (stable): a strong movement of fluid in one specific preferential direction;
- "D" = dry-out: when excessive heat power input causes a thermal crisis in at least one evaporator section.

Power-up phase (Q up)													Power-down phase (Q down)											
90°	-	-	S	C	C	C	C		C		C	C	C		C		C	C	C	C	O	S	S	90°
75°	-	-	S	S	S	S	C		C	C	D			D	D		C	C	C	O	S	S	-	75°
60°	-	-	-	C	C	C	C		C	C	D			D	D		C	C	O	O	S	S	-	60°
45°	-	-	S	S	O	C	C		D								C	C	C	O	S	S	-	45°
30°	-	S	S	S	C	C	C	D									O	C	C	O	S	S	-	30°
15°	-	S	S	S	S	O	D											O	O	S	S	S	-	15°
2.5°	-	O	O	O	D	D													O	O	O	-	-	2.5°
0°	-	-	-	-	-	-													-	-	-	-	-	0°
P[W]	10	20	30	40	60	90	120	140	160	180	210	260	210	180	160	140	120	90	60	40	30	20	10	P[W]

Table 1. Observed flow and activation conditions at varying degrees of inclination and heat power input. Empty fields are untested power levels and behaviour is inferred when possible.

Table 1 shows how an increase in inclination, and thus gravitational assistance, improves the flow conditions and broadens the operative range of the device. In nearly all experiments, the flow transitions from circulating to oscillatory for at least one full power step before eventually stopping. During circulation the fluid is always seen going preferentially from left to right of the observation field. However, also during circulation the fluid motion still maintains an oscillating component which causes brief pauses in movement between pulsations. This is visible in Figure 8: in the first three frames, circulation is rapid as shown by the rapid transition of bubble A, while in the last three frames the fluid decelerates, causing the next bubble marked B to briefly pause its movement.

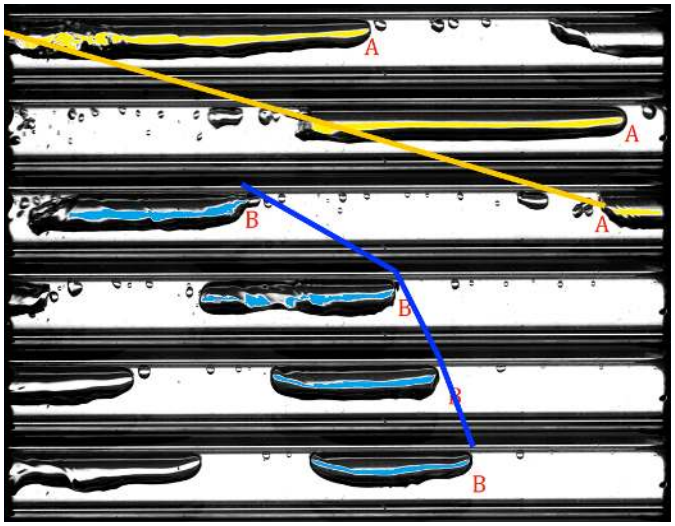

Figure 8. Flow circulation at 260 W in vertical orientation. The time interval between each image is 1/25th of a second and the flow bubble velocity varies from approximately 0.1 to 0.5 m/s.

Other interesting fluid flow phenomena were observed in the transparent section: larger bubbles travel fast enough that their trailing edge breaks up into smaller bubbles (Figure 9b). These smaller bubbles visibly shrink as the vapor condenses, and some of them collapse completely as a result (Figure 9a).

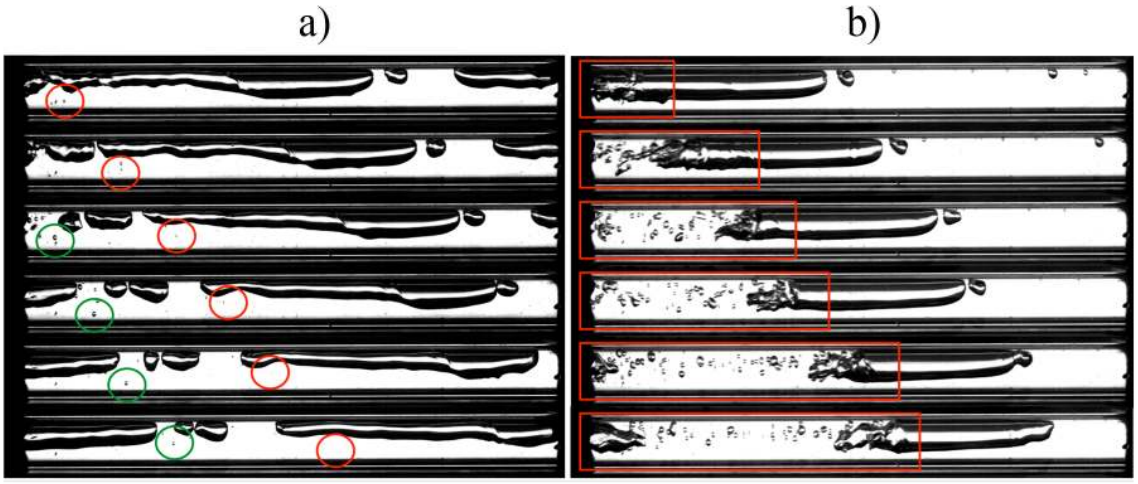

Figure 9. a) Small bubble condensation; b) Trailing edge break-up.

Before the start-up and during the shutdown, the other two visually characteristic flow types are stratified flow (Figure 10a), where from the only visible activity are ripples running along the liquid-vapor interface, and the oscillating bubble (Figure 10b). This last kind of motion is seen mostly during power-down: a single, elongated bubble oscillates back and forth in the condenser zone. In this condition, thermal resistance values still remain relatively low at about 0.3-0.34 K/W compared to 0.48-0.55 K/W for stratified flow.

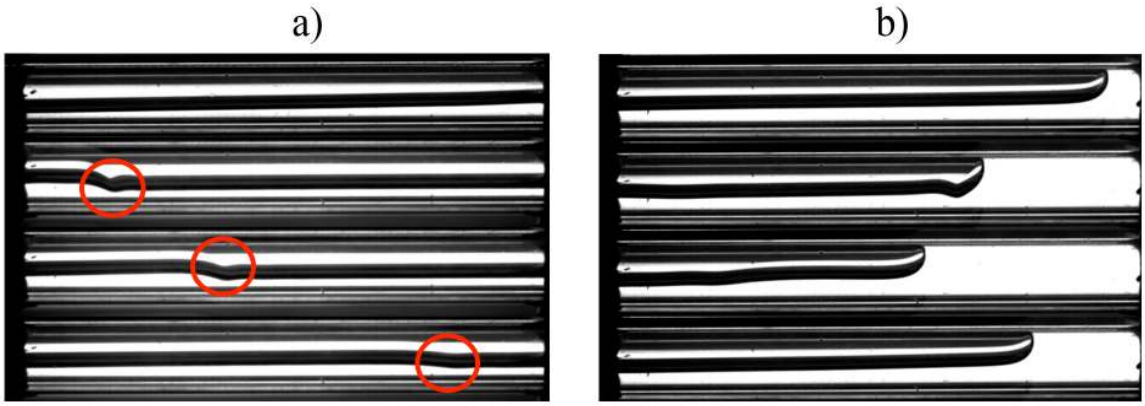

Figure 10. a) Stratified flow with highlighted ripples; b) Oscillating bubble.

CONCLUSIONS

A novel multi-evaporator, closed loop thermosyphon was tested with five heaters placed asymmetrically on an aluminium tube arranged on planar serpentine (3 mm internal diameter, filled with FC-72). The device's heat sink was cooled externally using ambient temperature air and the fluid flow conditions were observed through its transparent section, while a set of sixteen thermocouples was used to thermally characterize the device and to assess the beneficial effects of fluid circulation induced by the asymmetric heating.

The main outcomes are:

- The device does not exhibit hysteresis between power-up and power-down, but instead experiences penalized performance only during the first start-up from cold conditions. Once activation is achieved, power-up and power-down phases show similar performance.
- Inclination is a key parameter for dryout conditions, while also playing a less significant role in start-up. Raising the inclination (always in bottom heated mode) therefore effectively widens the device's operative power range, until peak performance is obtained in vertical orientation.
- The asymmetric placement of the heaters promotes a stable circulation of fluid in a preferential direction, directly observable from the glass tube that closes the loop in the condenser zone.
- Once the device is activated, thermal performance increases with power: above 3.3 W/cm^2, the equivalent thermal resistance drops below 0.34 K/W, reaching values of 0.1 K/W at 27 W/cm^2 in vertical conditions. For FC-72, this is a 57% gain compared to the pool boiling CHF limits.

NOMENCLATURE

Δh_{lv}	Latent heat of vapor,	[J/kg]
FR	Filling ratio	%
g	Gravity Acceleration,	[m/s2]
Ku	Kutateladze Number,	[-]
q''	Heat flux,	[W/cm^2]
$\dot{Q}$	Heat Input Power,	[W]
R_{eq}	Thermal Resistance,	[K/W]
T	Temperature ,	[°C]
ρ_l	Liquid Density,	[kg/m^3]

ρ_v	Vapor Density,	[kg/m^3]
σ	Surface Tension ,	[N/m]

ACKNOWLEDGEMENTS

The present work has been carried out in the framework of the Italian Space Agency (ASI) project ESA_AO-2009 entitled "Innovative two-phase thermal control for the International Space Station". The authors would like to thank Dr. Olivier Minster and Dr. Balazs Toth of the European Space Agency for their interest and support to the PHP activities and for the fruitful discussions. Also we acknowledge Ing. Paolo Emilio Battaglia of the Italian Space Agency for his administrative support. Finally we thank all the members of the Pulsating Heat Pipe International Scientific Team, for their contribution in pushing the PHP technology for space applications, with a particular gratitude to Prof. Sameer Khandekar, Dr. Vadim Nikolayev, Dr. Vincent Ayel and Prof. Marcia Mantelli.

REFERENCES

Esen M., Esen H., (2005). Experimental investigation of a two-phase closed thermosyphon solar water heater. Solar Energy, Vol.79, pp. 459-468.

Franco A., Filippeschi S. (2010). Experimental analysis of heat and mass transfer in small dimension, two phase loop thermosyphons, Heat Pipe Science and Technology, Vol. 2, pp. 163–182.

Franco A., Filippeschi S. (2012). Closed Loop Two-Phase Thermosyphon of Small Dimensions: a Review of the Experimental Results, Microgravity Sci. Technol. Vol. 24, pp.165–179.

Franco A., Filippeschi S. (2013). Experimental analysis of Closed Loop Two Phase Thermosyphon (CLTPT) for energy systems, Experimental Thermal and Fluid Science, Vol. 51, pp. 302–311.

Han L., Shi W., Wang B., Zhang P., Li X. (2013). Development of an integrated air conditioner with thermosyphon and the application in mobile phone base station. Int. J. of Refrigeration, Vol. 36, pp. 58-69.

Henry C.D., Kim J., Chamberlain B. (2004). Heater size and heater aspect ratio effects on sub-cooled Pool boiling heat transfer in low-g 3rd International Symposium on Two-Phase Flow Modeling and Experimentation Pisa, 22-24 September 2004.

Jouhara H., Robinson A. J. (2010). Experimental investigation of small diameter two-phase closed thermosyphons charged with water, FC-84, FC-77 and FC-3283. Applied Thermal Engineering, Vol. 30, pp. 201–211.

Katto, Y. (1985). Critical heat flux *Advances in Heat Transfer,* J. P. Hartnett and T. F. Irvine Editors, Academic Press, Vol. 17, pp. 1-64.

Kaminaga F., Matsumura K., Horie R., Takahashi A. (2012). A Study on Thermal Conductance in a Looped Parallel Thermosyphon, 16th International Heat Pipe Conference, Lyon, France, May 20-24.

Kim C.J., Yoo B.O., Park Y.J. (2005). Experimental Study of a Closed Loop Two-Phase Thermosyphon with Dual Evaporator in Parallel Arrangement. Journal of Mech. Sci. and Tech., Vol. 19(1), pp. 189-198.

Lahey R.T, Moody F.J., (1993). Thermal Hydraulic of Boiling Water Nuclear Reactor, American Nuclear Society.

Li J., Lin F., Niu G., (2014). An insert-type two-phase closed loop thermosyphon for split-type solar water heaters. Applied Thermal Eng., Vol.70, pp. 441-450.

Mameli M., Manno V., Filippeschi S., Marengo M. (2013). Thermal instability of a Closed Loop Pulsating Heat Pipe: Combined effect of orientation and filling ratio. Experimental Thermal and Fluid Science, Vol. 59, pp. 222–229.

Moradgholi M., Nowee S.M., Abrishamchi I., (2014). Application of heat pipe in an experimental investigation on a novel photovoltaic/thermal (PV/T) system. Solar Energy, Vol.107, pp. 82-88.

Perpinà X., Piton M,. Mermet-Guyennet M., Jorda` X., Millàn J. (2007). Local thermal cycles determination in thermosyphon-cooled traction IGBT modules reproducing mission profiles. Microelectronics Reliability, Vol. 47, pp. 1701–1706.

Reay D.A., Kew P.E., (2006). Heat Pipes, Fifth ed., Butterworth-Heinemann, Burlington, USA, 2006.

Sarno C., Tantolin C., Hodot R., Maydanik Y., Vershinin S., (2013). Loop thermosyphon thermal management of the avionics of an in-flight entertainment system, Applied Thermal Engineering Vol. 51, pp. 764-769.